6.a) Application to the polynuclear growth model in the droplet geometry.

6.a.1) Generalities on KPZ class in one dimension.

- Kardar-Parisi-Zhang (KPZ) wrote what they considered be an effective equation describing a stochastically growing interface $x \mapsto h(x,t)$:

(6.1)
$$\frac{\partial h(x,t)}{\partial t} = \nu \Delta h(x,t) + \frac{1}{2}\lambda (\nabla h(x,t))^2 + \eta(x,t), \qquad |\nabla h| \ll 1.$$

where : $\nu > 0$: is responsible for the smoothing (surface tension)

$\lambda > 0$: lateral growth

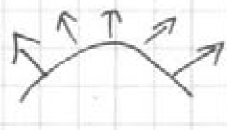

η : space-time local noise

- This equation comes from Taylor expansion of $v(\nabla h)$ for $|\nabla h| \ll 1$:

let $u = \nabla h$:
$$v(\nabla h) = v(0) + \underbrace{\frac{\partial v(0)}{\partial u} \cdot \nabla h}_{} + \frac{1}{2} \underbrace{\frac{\partial^2 v(0)}{\partial u^2}}_{\to\, \pm\lambda} \cdot (\nabla h)^2 + \cdots$$

Setting: $\tilde{h}(x,t) = h(x - \frac{\partial v(0)}{\partial u} \cdot t, t) - v(0) \cdot t$, this term disappears.

- Higher order terms do not matters for large t.

- (6.1) is the simplest continuous equation for an <u>irreversible</u>, <u>local</u>, <u>non-linear</u>, and <u>random</u> growth.

<u>Macroscopic behavior:</u> The smoothing mechanism makes the surface "macroscopically deterministic"; i.e.,

(6.2).
$$\lim_{t \to \infty} \frac{h(\xi \cdot t, t)}{t} = h_{ma}(\xi) \text{ is } \underline{\text{non-random}} \text{ (called limit shape).}$$

- <u>Fluctuations:</u> $\underline{H(x,t) := h(x,t) - t \cdot h_{ma}(x/t)}$.

- Fluctuation exponent: $1/3$: $|H(x,t)| \sim t^{1/3}$

- Correlation exponent : $2/3$: $|H(x,t) - H(x + t^{2/3}, t)| \sim t^{1/3}$.

. Scaling limit:

(6.3) $$h_t^{resc}(u) := \frac{h(\xi t + u t^{2/3}, t) - t \cdot h_{ma}\left(\frac{\xi t + u t^{2/3}}{t}\right)}{t^{1/3}}.$$

Q.: What is $\lim_{t\to\infty} h_t^{resc}(u)$? Does the limit process depends on the initial profile or not?

. To answer to these questions, one considers simplified models and try to get insights from the results proven.

Universality hypothesis: The statistical properties of the interface, for large growth time t, they should depends only on few global properties of the dynamics like:
- substrate dimension,
- locality of growth,
- symmetries,
- conservation laws.

. We consider the polynuclear growth model.

. The results so far proven indicates that, starting with an initial substrate without noise, e.g. $h(x,0)=0, \forall x$, the limit process

(6.4) $$\begin{cases} \lim_{t\to\infty} h_t^{resc}(u) = \kappa_v \cdot \mathcal{A}_2(u/\kappa_h), & \text{if } h''_{ma}(\xi)\neq 0 \ (\text{assuming } h''_{ma} \text{ smooth}). \\ \lim_{t\to\infty} h_t^{resc}(u) = \kappa_v \cdot \mathcal{A}_1(u/\kappa_h), & \text{if } h''_{ma}(\xi)=0 \text{ in a } \xi\text{-neighborhood}. \end{cases}$$

where κ_v, κ_h are vertical/horizontal scaling coefficients,

$\mathcal{A}_2$ is the Airy$_2$ Process and $\mathcal{A}_1$ is the Airy$_1$ process (which we did not see yet).

6.a.2) Discrete polynuclear growth model.

. It is a growth model with space and time discrete.

. The height function is integer-valued:

(6.5) $$h(x,t) \in \mathbb{Z}, \quad x \in \mathbb{Z},\ t \in \mathbb{N}.$$

. In the "droplet geometry" or "corner growth" is given as follows.

. Initial condition: $h(x,0)=0,\ x \in \mathbb{Z}$.

. Dynamics: $$h(x,t+1) = \max\{h(x-1,t),\ h(x,t),\ h(x+1,t)\} + \omega(x,t+1).$$

. The following special case is exactly solvable:

$\omega(x,t)=0$ if $t-x$ is odd or $|x|>t$.

Otherwise: $\omega(i-j, i+j-1) = w(i,j)$, $i,j \in \mathbb{N}_+^2$ are independent geometric random variables with parameter $0<a_i b_j<1$: i.e.,

(6.6) $$\mathbb{P}(w(i,j)=k) = (1-a_i b_j)\cdot(a_i b_j)^k, \quad k \geq 0.$$

. Later we will consider $a_i = b_j = \sqrt{q}$. Also, by taking $q \to 0$ and rescale space and time by $\frac{1}{\sqrt{q}}$ one gets Poisson points $\equiv$ continuous time PNG model.

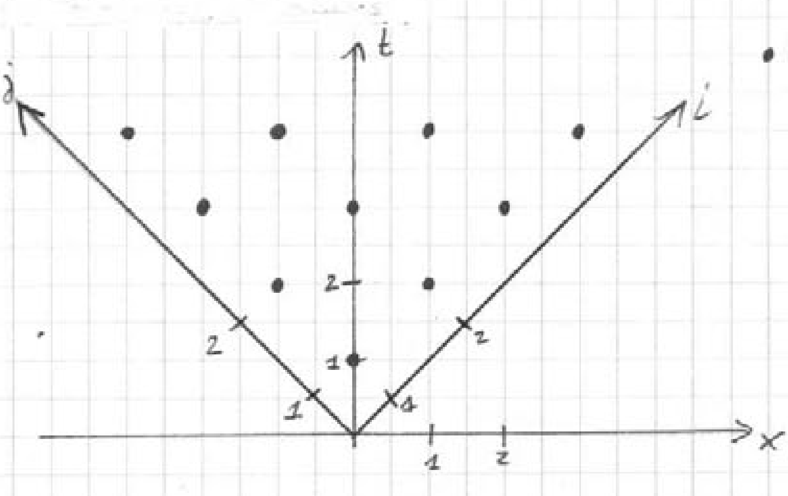

$\bullet \equiv (x,t)$ s.t. $\omega(x,t) \not\equiv 0$.

. let us see a couples of iterations.

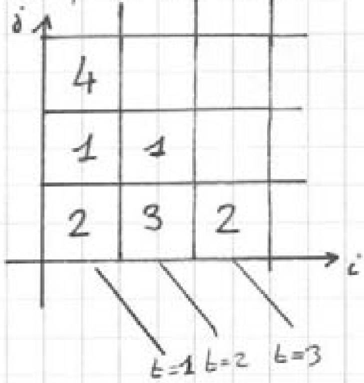

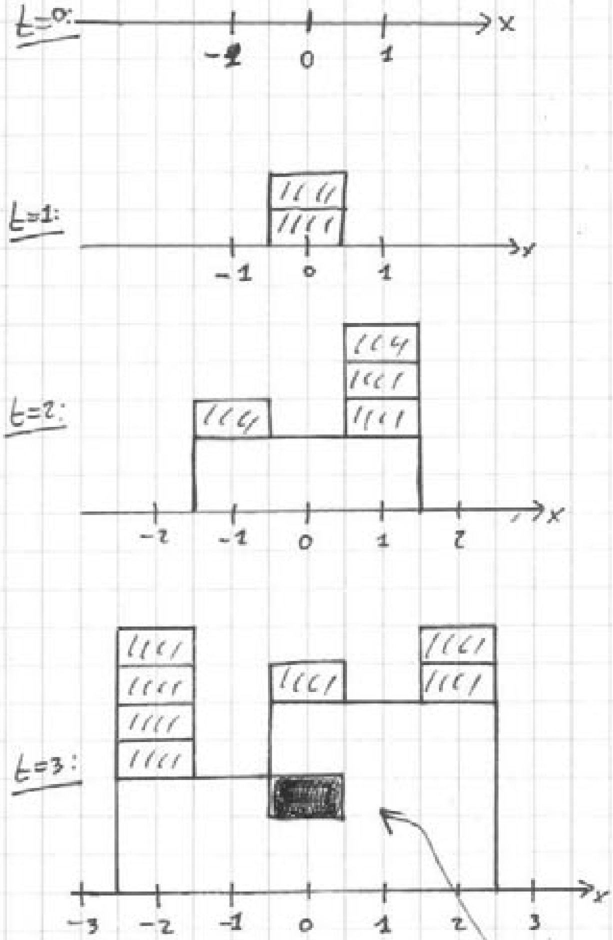

Multilayer PNG: . One sees that already at time $t=3$ two "islands" meet and "information" is lost: One can not recover the $w(i,j)$'s. So, even a nice measure on $w(i,j)$'s will not translate into a nice measure on the height function $h(x,t)$.

. This is avoided as follows: instead of a single height line, one has a set of lines $h_\ell(x,t)$, $\ell \le 0$.

- $h_0(x,t) \equiv h(x,t)$; $h_\ell(x,0) = -\ell$, $\ell \le 0$.
- $h_\ell(x,t)$ evolves like the dynamics of h_0 but the "nucleations", the $w_\ell(i,j)$, are just the blocks at level $\ell+1$ which annihilate, like the .

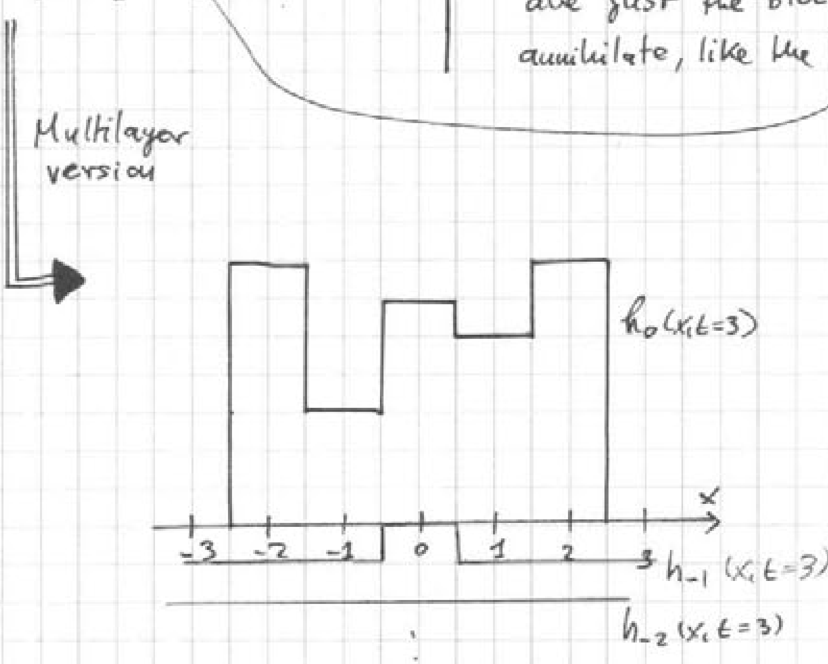

. Let us see how the <u>measure</u> on the $w(i,j)$ translates into the line ensemble.

$. \; w(1,1) : (a_1 \cdot b_1)^{w(1,1)}$

$. \; w(1,2) : (a_1 \cdot b_2)^{w(1,2)}$

$. \; w(2,1) : (a_2 \cdot b_1)^{w(2,1)}$

$\vdots$

<u>After time t:</u>

<u>$t=1$</u> $(a_1 \cdot b_1)^{w(1,1)}$

<u>$t=2$:</u> $(a_1 \cdot b_1)^{w(1,1)} \cdot (a_1 b_2)^{w(1,2)} \cdot (a_2 \cdot b_1)^{w(2,1)}$

<u>$t=3$:</u> . . .

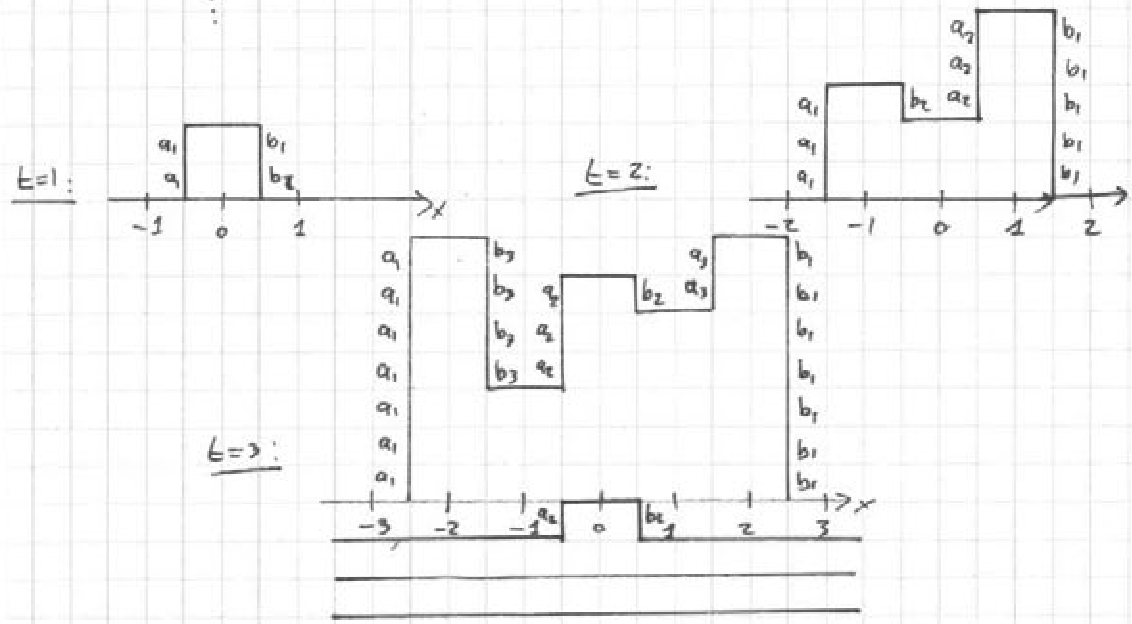

• So, we see that the mapping to the line ensemble keep a simple measure.

. By running the dynamics backwards, one can see that every non-intersecting line ensemble with $h_\ell(-t,t) = h_\ell(-t,t) = \ell$, $\ell \le 0$, it corresponds a unique configuration of the realization of the $\{w(i,j), \, i+j \le t+1\}$.

. <u>LGV scheme:</u> One can describe the line ensembles in the LGV scheme, as follows. The directed graph is between the vertices $(\mathbb{Z}+\frac{1}{2})\times\mathbb{Z}$. It is a "square graph" with the horizontal edges directed to the right and with weight 1, while the vertical ones alternating directed $\uparrow$ and $\downarrow$, with weights

$$\boxed{\begin{array}{ll} -t+\frac{1}{2}+2k: \; a_{k+1} & , \; k=1,\dots,t \\ t-\frac{1}{2}-2k: \; b_{k+1} & , \; k=1,\dots,t \end{array}}$$

as indicated in the above picture.

. To apply the LGV scheme, leading to a determinantal point process, we need to start with a finite number of lines, say N.

. At time t, they starts at $(-t,-\ell)_{\ell=0,\dots,N-1}$ and ends at $(t,\ell)_{\ell=0,\dots,N-1}$.

. <u>Remarks:</u> Actually there will be "a copy" of lines not straight at the bottom, but as $N\to\infty$, they becomes independent of the above ones (actually starting e.g. from $N>2t$).

. Now, we do not carry out the computations in this case. For $a_i=b_j=\sqrt{q}$, the details have been made by Johansson [math/0206208].

. <u>6.a.3) Continuous time PNG droplet.</u>

. To get back to the continuous time PNG, one considers
$$a_i=b_j=\sqrt{q}\,,\ \text{so},\ \mathbb{P}(w(i,j)=k)=(1-q)q^k,\ k\geq 0.$$

In particular $\mathbb{E}(w(i,j))=\frac{q}{1-q}=q+\mathcal{O}(q^2)$.

. Rescale space and time by $\frac{1}{\sqrt{q}}$:

(6.7) $$x=\left[\frac{X}{\sqrt{q}}\right],\ t=\left[\frac{T}{\sqrt{q}}\right].$$

. Then, $$\mathbb{E}\Big(\sum_{i,j\leq\frac{c}{\sqrt{q}}} w(i,j)\Big)=c^2(1+\mathcal{O}(q)) \text{ as } q\to 0.$$

. Most of the time, $w(i,j)=0$, rarely, $w(i,j)=1$ and essentially never $w(i,j)\geq 2$ (in any region $i,j\sim\frac{c}{\sqrt{q}}$).

So, in the limit $q\to 0$, and rescaling space and time by $\frac{1}{\sqrt{q}}$, one has <u>Poisson points with intensity one</u>.

. The LGV scheme describing the multilayer PNG droplet is the following:

. Consider N lines starting from:

$$(-t, \ell) \quad , \quad \ell = 0, \dots, -N+1$$

and arriving at

$$(t, \ell) \quad , \quad \ell = 0, \dots, -N+1,$$

with one-particle transition during "time interval" τ given by

$$P_\tau(x,y) = \langle y, e^{-\tau H} x \rangle \text{ , with} \tag{6.8}$$

$$H\psi(n) = -(\psi(n+1) + \psi(n-1)) \quad , \quad \psi \in \ell^2(\mathbb{Z}).$$

. In other words, $$P_\tau(x,y) = \frac{1}{2\pi i} \oint_{\Gamma_0} \frac{dz}{z^{y-x+1}} \cdot e^{\tau(z + \frac{1}{z})} . \tag{6.9}$$

. <u>A picture of the LGV scheme:</u>

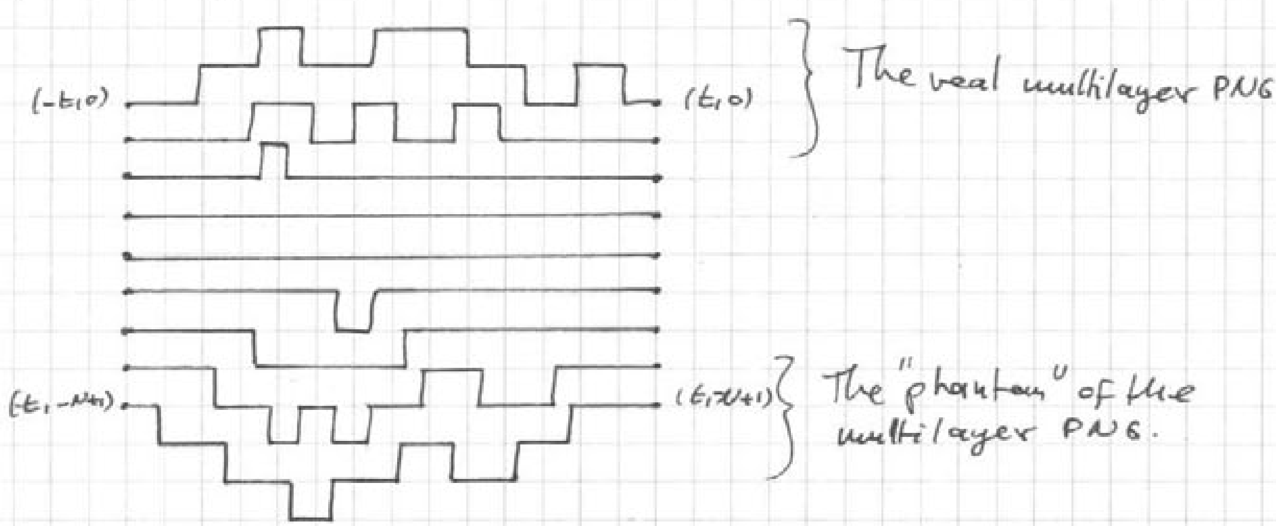

. When N becomes large, the real and the "phantom" multilayers become independent. So, if we focus in any region bounded from below, after the $N \to \infty$ limit we have <u>exactly</u> the multilayer PNG with ∞-many layers.

. Measure: m-points at $-t < \tau_1 < \tau_2 < \dots < \tau_m < t$
is given by

$$(6.10)\quad \text{const}\times \det\left(P_{t+\tau_1}(-i+1, x_j^1)\right)_{1\le i,j\le N} \cdot \left(\prod_{k=1}^{m-1} \det\left(P_{\tau_{k+1}-\tau_k}(x_i^k, x_j^{k+1})\right)_{1\le i,j\le N}\right) \cdot \det\left(P_{t-\tau_m}(x_i^m, -j+1)\right)_{1\le i,j\le N}.$$

. By Proposition 19, we have the Kernel

$$(6.11)\quad K_N(t_1 x_1; t_2 x_2) = -P_{t_2-t_1}(x_1,x_2)\cdot \mathbb{1}_{[t_2>t_1]} + \sum_{i,j=1}^{N} P_{t-t_2}(x_2,-i+1)\cdot [A_N^{-1}]_{i,j}\cdot P_{t+t_1}(-j+1, x_1)$$

where $[A_N]_{i,j} = P_{2t}(-i+1,-j+1)$, $1\le i,j\le N$.

. Remarks on the $N\to\infty$ limit: ⓐ $P_{t-t_2}(x_2,-i+1)$ goes exponentially to zero as $i\to\infty$,
ⓑ $P_{t+t_1}(-j+1,x_1)$ " " " $j\to\infty$,
ⓒ $A_N(i,j)$ " " " $|i-j|\to\infty$.

$$A_N = \begin{pmatrix} A_N(1,1) & \cdots & A_N(1,N) \\ \vdots & & \vdots \\ A_N(N,1) & \cdots & A_N(N,N) \end{pmatrix}$$

. From ⓐ and ⓑ, one need to prove that
for any given m, the $m\times m$ block of $[A_N^{-1}]_{1\le i,j\le m} \xrightarrow{N\to\infty} [A_\infty^{-1}]_{1\le i,j\le m}$,
and that the remainder of the inverse is not exploding.

. The half-infinite matrix has an inverse which we can compute.
One then uses $A_N\cdot A_\infty^{-1} = \mathbb{1} + R_N \Rightarrow A_N^{-1} = (\mathbb{1}+R_N)^{-1} A_\infty$.
(the $N\times N$ matrix-block of the A_∞^{-1} matrix)

. One has to compute A_∞^{-1}, then $A_N\cdot A_\infty^{-1}$ and see that R_N is small as $N\to\infty$.

. We do not give more details here, but in this case can be done.

. After having taken the $N\to\infty$ we have a kernel given by:

(6.12) $$K(t_1x_1;t_2x_2) = -P_{t_2-t_1}(x_1x_2)\,\mathbb{1}_{[t_2>t_1]} + \sum_{i,j=1}^{\infty} P_{t-t_2}(x_2,-i+1)\cdot[A_\infty^{-1}]_{ij}\cdot P_{t+t_1}(-j+1,x_1).$$

(6.13) . $A_\infty = [A]_{1\le i,j\le\infty}$ with $A_{ij} = \frac{1}{2\pi i}\oint_{\Gamma_0} dz\,\frac{e^{2t(z+z^{-1})}}{z^{i-j+1}}$.

. Its inverse is given by:

(6.14) $$[A_\infty^{-1}]_{ij} = \sum_{k\geq 1}\frac{1}{(2\pi i)^2}\cdot\oint_{\Gamma_0} dw\,\frac{e^{-2tw}}{w^{i-k+1}}\cdot\oint_{\Gamma_0} dz\,\frac{e^{-2tz^{-1}}}{z^{k-j+1}}.$$

. To obtain this, remark that A is the product of two triangular matrices:

$$A_{ij} = \sum_{k\geq 1}\left(\frac{1}{2\pi i}\oint_{\Gamma_0} dz\,\frac{e^{2tz^{-1}}}{z^{i-k+1}}\right)\left(\frac{1}{2\pi i}\oint_{\Gamma_0} dw\,\frac{e^{2tw}}{w^{k-j+1}}\right)$$

$$= \frac{1}{(2\pi i)^2}\cdot\underbrace{\oint_{\Gamma_0} dz\oint_{\Gamma_0} dw}_{|z|<|w|}\,\frac{e^{2tz^{-1}}\cdot e^{2tw}}{z^{i+1}}\cdot w^{j-1}\underbrace{\sum_{k\geq 1}\left(\frac{z}{w}\right)^k}_{=\frac{z}{w}\cdot\frac{w}{w-z}}$$

$$\overset{\text{Simple pole at } w=z}{=} \frac{1}{2\pi i}\oint_{\Gamma_0} dz\,\frac{e^{2t(z^{-1}+z)}}{z^{i-j+1}}.$$

. Thus, the inverse is the product of the inverses with exchanged order:

$$[A_\infty^{-1}]_{ij} = \sum_{k\geq 1}\frac{1}{2\pi i}\oint_{\Gamma_0} dw\,\frac{e^{-2tw}}{w^{i-k+1}}\cdot\frac{1}{2\pi i}\oint_{\Gamma_0} dz\,\frac{e^{-2tz^{-1}}}{z^{k-j+1}}.$$

. Therefore, the kernel is given by:

(6.15) $$\boxed{K(t_1x_1;t_2x_2)} = -\frac{1}{2\pi i}\oint_{\Gamma_0} dz\, e^{(t_2-t_1)(z+z^{-1})}\,\mathbb{1}_{[t_2>t_1]}$$

$$+ \sum_{k\geq 0}\frac{1}{2\pi i}\oint_{\Gamma_0} dz\,\frac{e^{(t-t_2)z^{-1}-(t+t_2)z}}{z^{-k-x_2+1}}\cdot\frac{1}{2\pi i}\oint_{\Gamma_0} dw\,\frac{e^{(t+t_1)w-(t-t_1)/w}}{w^{x_1+k+1}}$$

$$= -\frac{1}{2\pi i}\oint_{\Gamma_0} dz\, e^{(t_2-t_1)(z+z^{-1})}\,\mathbb{1}_{[t_2>t_1]} + \frac{1}{(2\pi i)^2}\cdot\oint_{\Gamma_0} dz\oint_{\Gamma_{0,z}} dw\,\frac{e^{(t-t_2)z^{-1}-(t+t_2)z}}{e^{(t-t_1)w^{-1}-(t+t_1)w}}\cdot\frac{z^{x_2-1}}{w^{x_1}}\cdot\frac{1}{w-z}.$$

- Kernel given in terms of Bessel functions.

. For $b \geq a$ and $n \in \mathbb{Z}$: $\displaystyle\frac{1}{2\pi i}\oint_{\Gamma_0}\frac{dz}{z}\,\frac{e^{b(z-z^{-1})}\cdot e^{a(z+z^{-1})}}{z^n} = \left(\frac{b+a}{b-a}\right)^{n/2} J_n\left(2\sqrt{b^2-a^2}\right)$

where J_n are the standard Bessel functions.

. Then, the kernel writes:

$$(6.16)\quad K(t_1 x_1; t_2 x_2) = \begin{cases} \displaystyle\sum_{\ell \leq 0} \left(\frac{t-t_2}{t+t_2}\right)^{\frac{x_2-\ell}{2}} \cdot \left(\frac{t+t_1}{t-t_1}\right)^{\frac{x_1-\ell}{2}} \cdot J_{x_2-\ell}\left(2\sqrt{t^2-t_2^2}\right) J_{x_1-\ell}\left(2\sqrt{t^2-t_1^2}\right), & \text{for } t_2 \leq t_1, \\ \displaystyle\sum_{\ell > 0} \quad '' & \text{for } t_2 > t_1. \end{cases}$$

6.a.4) Edge scaling and $Airy_2$ process.

. We want to study: $\displaystyle h_t^{edge}(u) := \frac{h(ut^{2/3}, t) - 2t + u^2 t^{1/3}}{t^{1/3}}$

. So, the rescaled point process of $\eta_t(x,s)$, the one associated to the multilayer, is $\eta_t^{edge}(u,s) = t^{1/3}\cdot\eta_t\left(ut^{2/3}, [2t - u^2 t^{1/3} + st^{1/3}]\right)$,

and the associated kernel:

$$K_t^{edge}(u_1 s_1; u_2 s_2) = t^{1/3}\cdot K\left(u_1 t^{2/3}, [2t - u_1^2 t^{1/3} + s_1 t^{1/3}]; u_2 t^{2/3}, [2t - u_2^2 t^{1/3} + s_2 t^{1/3}]\right)$$

. One analyzes K_t^{edge} with steep descent method and obtain:

$$(6.17)\quad \lim_{t\to\infty} K_t^{edge}(u_1 s_1; u_2 s_2) \overset{\text{(conjugation)}}{=} \frac{+1}{(2\pi i)^2}\cdot\int_{\gamma_1} dw \int_{\gamma_2} dz\, \frac{e^{\frac{z^3}{3} + u_2 z^2 + (u_2^2 - s_2)z}}{e^{\frac{w^3}{3} + u_1 w^2 + (u_1^2 - s_1)w}}\cdot\frac{1}{z-w}$$

where

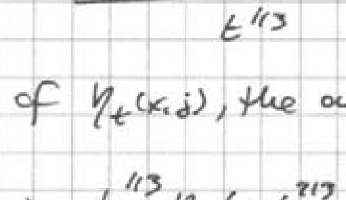

$$- \frac{\mathbb{1}[u_1 < u_2]}{2\pi i}\cdot\int_{i\mathbb{R}} dw\, e^{(u_2 - u_1)w^2 + (u_2^2 - u_1^2 - s_2 + s_1)w}$$

$$= K_{A_2}(u_1 s_1; u_2 s_2).$$

. By appropriate control in the tails (largest), so that the Fredholm determinant converges too, one then gets:

Theorem 25: In the sense of finite-dimensional distributions,

$$\lim_{t\to\infty} h_t^{edge}(u) = \mathcal{A}_2(u). \qquad (6.19)$$

. Remark: . As shown by Johansson in the context of discrete time PNG,

$$\mathbb{P}\left(\sup_{u\in\mathbb{R}}\left(\mathcal{A}_2(u)-u^2\right)\leq s\right) = F_1(s).$$

. So, if the process h_t^{edge} is tight, then

$$\lim_{t\to\infty} \mathbb{P}\left(\sup_{u\in\mathbb{R}} \frac{h(u\ \ ,t)-2t}{t^{1/3}} \leq s\right) = F_1(s).$$

. Remark: The analogue of the Airy$_2$ process for flat PNG, defined by removing the constraint that the poisson points occurs only on $|x|\leq t$.

$\Rightarrow$ $h_{ma}(\xi) = 2$ and

$$\lim_{t\to\infty} h_t^{edge}(u) = 2^{1/3}\mathcal{A}_1(2^{-2/3}u)$$

: the Airy$_1$ Process given in the next section.

Discrete time PNG $\leftrightarrow$ Directed Polymers

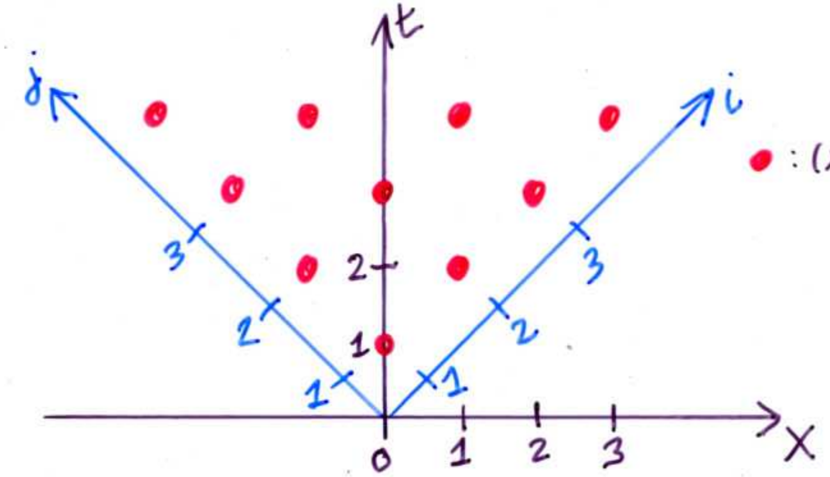

$\bullet$: (x,t) s.t. $\omega(x,t) \not\equiv 0$.

I.C.: $h(x, t=0) = 0, \ \forall x \in \mathbb{Z}$

Dynamics: $h(x, t+1) = \max\{h(x-1,t), h(x,t), h(x+1,t)\} + \omega(x, t+1)$

"energy" $\updownarrow$ $\equiv$ "length" of the longest directed polymer.

. Particular (solvable) case:

$$\begin{cases} \omega(x,t) = 0 & \text{if } t-x \text{ is odd or } |x| > t \\ \omega(x,t) \not\equiv 0 & \text{otherwise, with} \end{cases}$$

$\omega(i-j, i+j-1) = w(i,j)$, $i,j \in \mathbb{N}_+^2$ i.i.d. geometric random variables:

$$\mathbb{P}(w(i,j) = k) = (1 - a_i b_j)\cdot(a_i b_j)^k, \ k \geq 0.$$

Example:

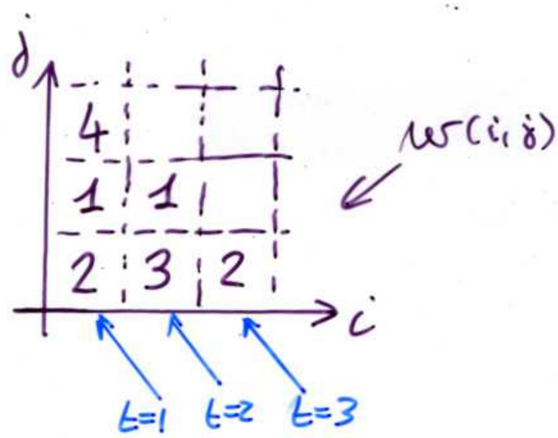

Height function:

$t=0$:

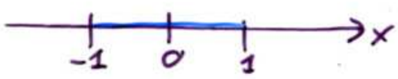

$t=1$:

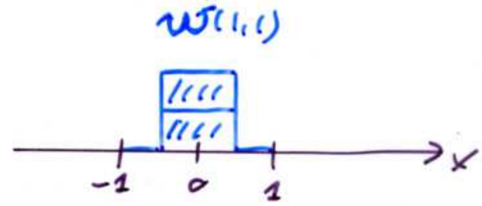

$t=2$:

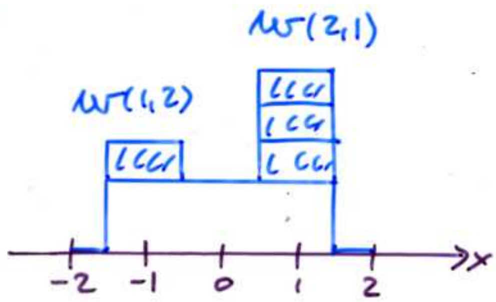

$t=3$:

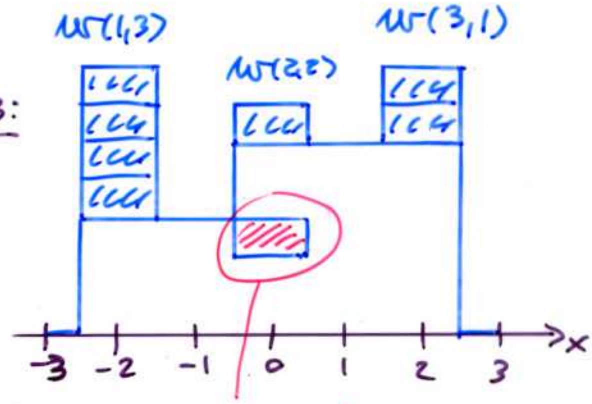

Intersection $\equiv$ Lost of information.

Multilayer PNG:

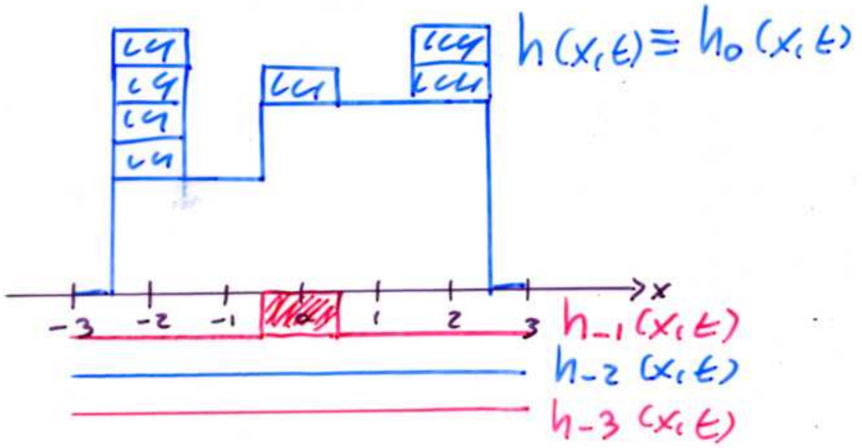

Measure: from $w(i,j)$ to multilayer.

t=1: $w(1,1) \Rightarrow$ weight $(a_1 \cdot b_1)^{w(1,1)} = a_1^2 \cdot b_1^2$

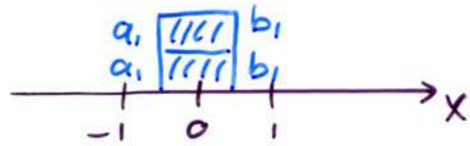

t=2: weight $(a_1 \cdot b_1)^{w(1,1)} \cdot (a_1 b_2)^{w(1,2)} \cdot (a_2 b_1)^{w(2,1)}$

$$= a_1^3 \cdot b_2^1 \cdot a_2^3 \cdot b_1^5$$

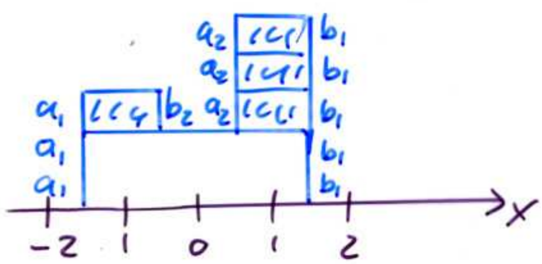

t=3: weight $=$ (weight at $t=2$) $\cdot (a_1 b_3)^4 \cdot (a_2 b_2)^1 \cdot (a_3 b_1)^2$

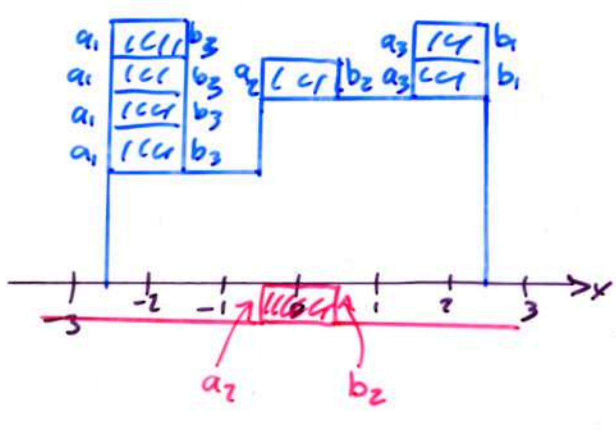

LGV scheme: example for $t=3$.

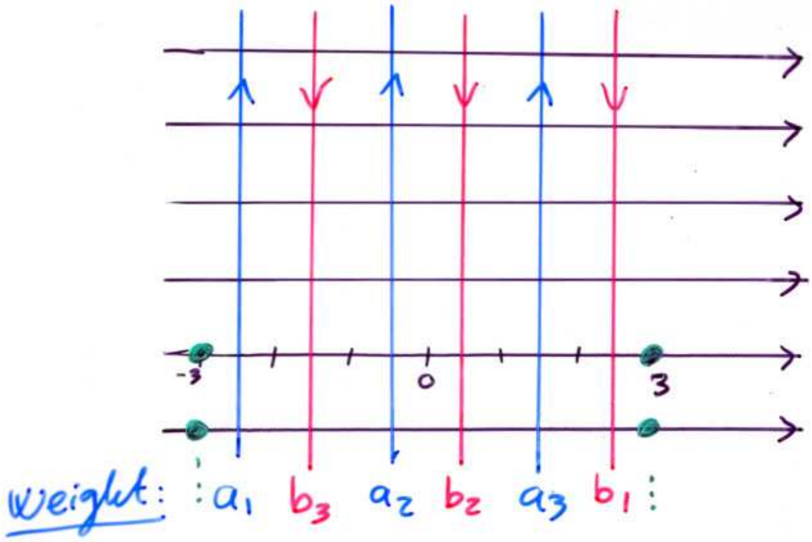

$\longrightarrow$: oriented to the right, weight $\equiv 1$.

- Non-intersecting lines from $(-t, \ell)$, $\ell \leq 0$ to (t, ℓ), $\ell \leq 0$.

- Steps: 1) Consider N non-intersecting lines on LGV and compute the Kernel.

  2) Take $N \to \infty$ for finite t

  3) Take $t \to \infty$ under appropriate scaling limit.

- For $a_i = b_i = \sqrt{q}$: Top line $\equiv$ PNG height function converges to the Airy$_2$ Process [Johansson]

5

• Continuous time PNG

• $a_i = b_i = \sqrt{q} \Rightarrow \mathbb{P}(w(i,j)=k) = (1-q)q^k, \quad k \geq 0.$

• Take $q \to 0$ and rescale space and time:

$$x = \left[\frac{X}{\sqrt{q}}\right], \quad t = \left[\frac{T}{\sqrt{q}}\right].$$

• When $q \to 0$: $\begin{cases} w(i,j) = 0 \text{ most of the time,} \\ w(i,j) = 1 \text{ with proba.} \sim q, \\ w(i,j) \geq 2 \quad \text{"} \quad \text{"} \quad q^2\text{: } \underline{\text{irrelevant.}} \end{cases}$

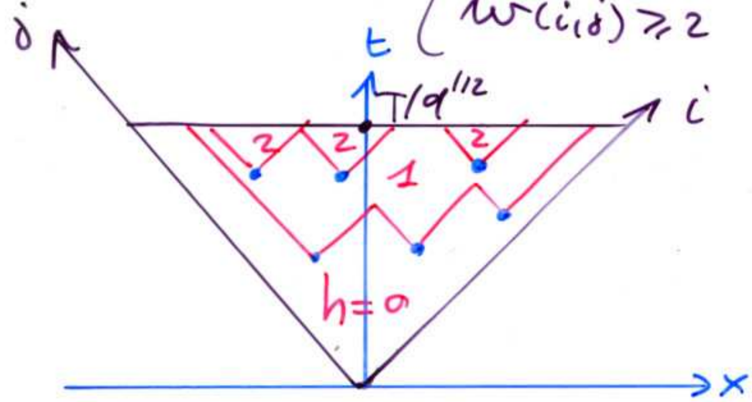

• ≡ $w(i,j) = 1$: Poisson Points with intensity one.

. Results: [Prähofer–Spohn'02]

① $$\mathbb{P}\left(\bigcap_{i=1}^{m}\{h(X_i,T) \leq a_i\}\right) = \det\left(\mathbb{1} - \chi_a K_T^{PNG} \chi_a\right)$$

$L^2(\{X_1,\dots,X_m\}\times\mathbb{R})$

with $\chi_a(X_i,z) = \mathbb{1}_{[z>a_i]}$, and

($J_n(x)$: Bessel functions)

$$K_T^{PNG}(X_1,h_1;X_2,h_2) = \begin{cases} \displaystyle\sum_{e\geq 0}\left(\frac{T-X_2}{T+X_2}\right)^{\frac{h_2+e}{2}} J_{h_2+e}\left(2\sqrt{T^2-X_2^2}\right) \\ \quad \cdot \left(\frac{T+X_1}{T-X_1}\right)^{\frac{h_1+e}{2}} J_{h_1+e}\left(2\sqrt{T^2-X_1^2}\right), \\ \quad \text{if } -T \leq X_2 \leq X_1 \leq T \\ \displaystyle -\sum_{e<0}(\quad \text{"} \quad), \quad \text{if } T \geq X_2 > X_1 \geq -T. \end{cases}$$

② Edge scaling:

$$h_T^{edge}(u) := \frac{h_0(uT^{2/3},T)-(2T-u^2T^{1/3})}{T^{1/3}}$$

$$\boxed{\lim_{T\to\infty} h_T^{edge}(u) = \mathcal{A}_2(u).}$$

. Flat PNG:

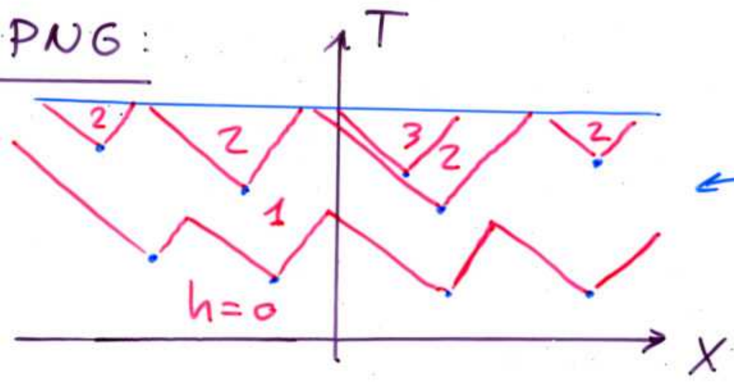

← Poisson Points ~~not~~ restricted to $|x| \le T$ anymore.

. Results: [Borodin-Ferrari-Sasamoto '07]

① $\mathbb{P}\left(\bigcap_{i=1}^{m}\{h(x_i,T)\le a_i\}\right) = \det(\mathbb{1}-\chi_a K_T^{flat}\chi_a)$

with $K_T^{flat}(x_1,h_1;x_2,h_2) = -I_{|h_1-h_2|}(2(x_2-x_1))\mathbb{1}_{[x_2>x_1]}$

$$+\left(\frac{2T+x_2-x_1}{2T-x_2+x_1}\right)^{\frac{h_1+h_2}{2}} \cdot J_{h_1+h_2}\left(2\sqrt{4T^2-(x_2-x_1)^2}\right) \cdot \mathbb{1}_{[2T\ge|x_2-x_1|]}$$

② Edge scaling:

$$h_T^{edge}(u) := \frac{h(uT^{2/3},T)-2T}{T^{1/3}}$$

$$\boxed{\lim_{T\to\infty} h_T^{edge}(u) = 2^{1/3}\cdot\mathcal{A}_1(2^{-2/3}\cdot u)}$$